Ammonia Inversion Spectrum

Alex Leonardi[1, 2, *] and Inko Bovenzi[1, 3, †]

[1] *Department of Physics, Harvard University, Cambridge, Massachusetts 02138, USA*
[2] *Department of Mathematics, Harvard University, Cambridge, Massachusetts 02138, USA*
[3] *Department of Computer Science, Harvard University, Cambridge, Massachusetts 02138, USA*

(Dated: May 24, 2025)

We measure the inversion spectrum of the ammonia molecule, detecting the five strongest absorption lines using microwave spectroscopy. By plotting the intensity of applied microwaves as a function of frequency on an oscilloscope and sweeping relevant frequencies, we observe dips at frequencies associated with ammonia inversion. Our results for inversion frequencies and relative intensities line up well with the accepted values in the literature. The strongest absorption line displayed hyperfine splitting. Secondly, we measure the broadening of inversion lines as a function of pressure, finding a linear relationship between pressure and inversion line width for three absorption lines. The results show a demonstration of the principles of quantum tunneling. Studies of the physics of ammonia inversion have application to the development of ammonia masers.

I. INTRODUCTION

In 1964, Charles Townes, Aleksandr M. Prokhorov, and Nicolay Basov shared the Nobel Prize in physics for their contributions to quantum electronics based on the development of masers and lasers [1]. Masers were originally pioneered using ammonia to generate coherent beams of microwaves and in this paper we examine the inversion spectrum of ammonia, which is the basis for understanding and constructing ammonia masers.

Ammonia is the trigonal pyramidal molecule NH_3, where nitrogen experiences a double-well potential due to three hydrogen atoms at the base of the pyramid configuration. Ammonia inverts when nitrogen tunnels through the base, splitting the ground state into two distinct energy levels. In the classical view, we picture nitrogen at a given time being located on a specific side, either left or right, of the double potential well [2]. The quantum mechanical view assigns probabilities to being on one side or the other at a particular time, with the energy difference in the states being the same as the energy of a photon that has a frequency of $\sim$ 24,000 megacycles per second [2].

The inversion spectrum of ammonia occurring at room temperature then corresponds to these different rotational states. We identify lines that correspond to the frequency for these transitions and further investigate the induced hyperfine splitting and pressure broadening. Hyperfine splitting is the presence of additional lines in the inversion spectrum arising from the energy change due to interaction between the nuclear quadrupole moment and the electrostatic potential. We observe pressure broadening by varying the pressure of ammonia in our system, where the signal amplitude correspondingly varies, and we see changes in the frequency correspond to more or less collisions between molecules. We denote rotational states using their associated angular momentum quantum numbers J and K and while a molecule may transition between the two energy levels, its rotational state remains the same [3]. The angular momentum quantum numbers J and K are related to the total angular momentum P in the following manner,

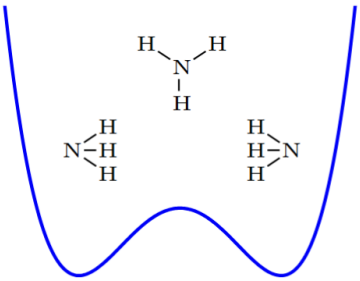

FIG. 1. Ammonia's double potential well. The nitrogen atom can jump the gap between the two wells when absorbing microwaves of a certain frequency. The state on the left is taken as $|1\rangle$ and the one on the right is $|2\rangle$.

$$P^2 = J(J+1)\hbar^2 \tag{1}$$

$$P_z^2 = K^2\hbar^2 \tag{2}$$

where $J \in \mathbb{Z}$ and $K \in \{-J, -J+1, \ldots, J-1, J\}$ [4].

From the experiment conducted by Charles Townes in [5], we first focus on $(J, K) = (3, 3)$ because it has the highest reported intensity. After identifying the desired behavior due to the microwave spectroscopy data displayed on the oscilloscope, we collect data for the remainder of the (J, K) table to plot the inversion spectrum of ammonia.

* alexleonardi@college.harvard.edu
† ibovenzi@college.harvard.edu

II. PRELIMINARIES ON THE GENERAL THEORY OF THE ABSORPTION OF LIGHT BY A MOLECULAR OR ATOMIC SYSTEM

Following the discussion in [6], in this section we develop the theory for the absorption of light by ammonia and for the ammonia microwave amplification by stimulation emission of radiation (ammonia maser). The maser generates electromagnetic radiation using the ammonia molecule [6].

We have that the superposition of states for the ammonia molecule is,

$$|\psi\rangle = c_1 |1\rangle + c_2 |2\rangle , \tag{3}$$

where $c_1,\ c_2$ are the probabilities associated with being in either the left state $|1\rangle$ or the right state $|2\rangle$. See Fig. 1 for a visual depiction of these states in the double potential well.

We consider the general dynamical equation in quantum mechanics,

$$i\hbar \frac{dC_i(t)}{dt} = \sum_j H_{ij}(t) C_j(t) \tag{4}$$

where H_{ij} are entries in the Hamiltonian matrix of the system and C_j are the probabilities associated with the state. For the two level system we examine for ammonia, we consider the Hamiltonian,

$$\begin{pmatrix} H_{11} & H_{12} \\ H_{21} & H_{22} \end{pmatrix} = \begin{pmatrix} E_0 & -A \\ -A & E_0 \end{pmatrix} \tag{5}$$

The solution,

$$c_1 = \frac{a}{2} e^{-(i/\hbar)(E_0 - A)t} + \frac{b}{2} e^{-(i/\hbar)(E_0 + A)t} \tag{6}$$

$$c_2 = \frac{a}{2} e^{-(i/\hbar)(E_0 - A)t} - \frac{b}{2} e^{-(i/\hbar)(E_0 + A)t} \tag{7}$$

then corresponds to the states $|\psi_I\rangle$ and $|\psi_{II}\rangle$ with energies $E_I = E_0 + A$ and $E_{II} = E_0 - A$. These are the stationary states corresponding to when $a = 0$ or $b = 0$, respectively, since $a = 0$ gives us that both terms have the frequency $\omega_b = (E_0 + A)/\hbar$ and amplitudes such that $c_1 = -c_2$, whereas $b = 0$ implies both terms have the same frequency $\omega_a = (E_0 - A)/\hbar$ and the same amplitude.

The mathematics describing the ammonia molecule's states is similar to the description of a pair of pendulums, where the frequency ω_a corresponds to the case where the pendulums oscillate together as compared to the frequency ω_b, when the pendulums oscillate in opposing directions.

If we consider exciting the electrons in an atom, then we need light in the visible or ultraviolet range. Additionally, infrared light excites vibrations of the molecules.

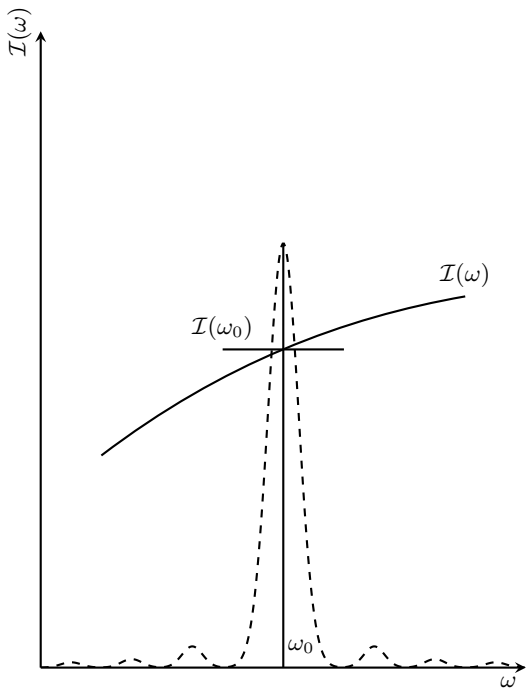

FIG. 2. Approximating the spectral intensity $\mathcal{I}(\omega)$ using $\mathcal{I}(\omega_0)$. This graph can also be found as Fig. 9-8 in [6].

For exciting rotations, we require light in the far infrared. In the case of ammonia, $E_I - E_{II} = 2A$ turns out to be in the microwave range, which is beyond infrared. Previous experiments on the ammonia inversion spectrum, including [5], have found that $f \sim 24,000$ GHz satisfies $2A = hf$.

As derived in [6], we can calculate the probability for a transition between the states $|\psi_I\rangle$ and $|\psi_{II}\rangle$ with the absorption of the electromagnetic wave as,

$$P(I \to II) = 4\pi^2 \left[\frac{\mu^2}{4\pi\epsilon_0 \hbar^2 c} \right] \mathcal{I}(\omega_0) T, \tag{8}$$

where μ is the electric dipole moment, $\mathcal{I}(\omega_0)$ is the spectral intensity evaluated at the resonant frequency ω_0, and T is the time duration. Fig. 2 depicts the shape of the spectral intensity and shows how to approximate it using the value of $\mathcal{I}$ at ω_0. Following the discussion of Eqn. 8 in [6], we gather that the frequency must be almost exactly ω_0 for the transition to likely occur. We do exactly this by employing the waveguide to precisely choose $I(\omega)$ close to the resonance frequency of the cavity. We note that experimentally we can tune the resonance frequency of the cavity.

III. SETUP

We used a Gunn diode oscillator (GDO) to generate microwaves and a sawtooth modulation supply to sweep through a range of frequencies. For coarse frequency

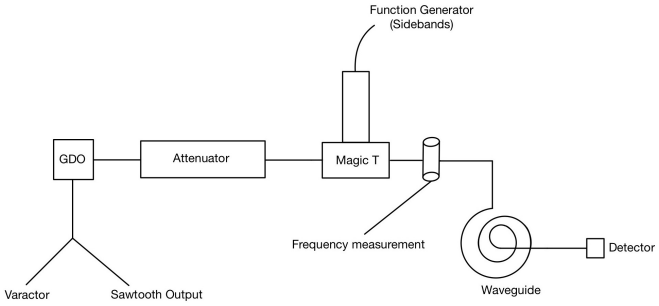

FIG. 3. Schematic of experimental setup. Note that the Magic T also contains a knob (a fourth port that is not pictured here) that can be adjusted to control the length of the waveguide. Changing the length of the waveguide results in the microwaves either constructively interfering more, or leads to more destructive interference. For our purposes, we aim to have stronger microwave signals and so we adjusted this length such that the microwaves experienced the most constructive interference possible.

modulation, the GDO has a direct frequency knob, but we made fine changes to the frequencies using the varactor on the sawtooth box.

The microwaves moved through an attenuator that limited their strength before entering the magic T. We introduced sidebands on either side of the central frequency being swept to the Magic T to aid in frequency measurements in the pressure broadening experiment. Because these side bands were a fixed frequency away fro the center of the signal, they allowed us to convert from time measurements on the oscilloscope to frequencies. Before every run, we pumped all excess air and ammonia out of the system and then added ammonia until reaching the desired pressure of 100 mTorr.

We plugged two outputs into the oscilloscope: the microwave power read by the end detector and the output from "trigger" on the sawtooth box. We used the trigger output to fix the waveform on the oscilloscope and averaged over 64 waveforms on the display to minimize the effects of noise.

We measured the frequencies of the inversion lines using the frequency absorption meter, or cavity. Turning the meter changes the size of the cavity such that different frequencies resonate in the chamber and are absorbed. Thus, the cavity creates a dip at a given frequency if that frequency is in the swept range.

IV. AMMONIA INVERSION LINES

A. Results

Table I shows the J and K values for each of the ammonia inversion lines we found, the frequencies we detected, their accepted frequency values [5], and the residuals. In general, our results were very closely in line with the accepted values, with an average miss of 11 MHz,

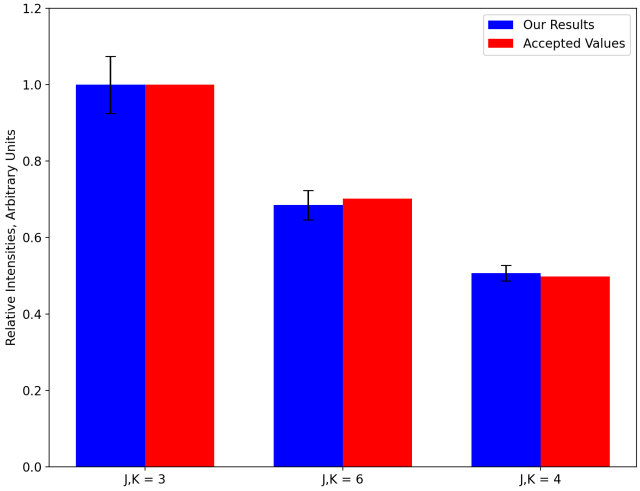

FIG. 4. Relative intensities of the three absorption lines with credible measurements. Our data closely aligns with the accepted values [5]. The error bars represent two sigma.

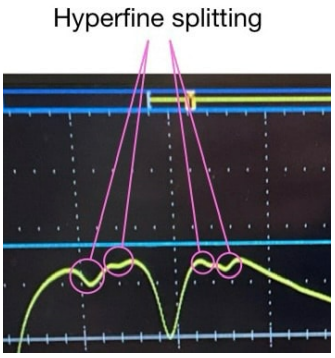

FIG. 5. Hyperfine splitting seen on the (3,3) absorption line.

which amounts to a .05% measuring error for a typical frequency. Though the lines were more difficult to perceive at lower relative intensities, our residuals did not seem to rise substantially for the later lines.

(J, K)	Experiment	Accepted	Residual (MHz)
(3, 3)	23.878(20)	23.870	8
(6, 6)	25.061(20)	25.046	15
(4, 4)	24.141(20)	24.137	4
(3, 2)	22.830(20)	22.840	-10
(2, 2)	23.740(20)	23.722	18

TABLE I. Experiment and accepted values. All measurements in GHz unless otherwise noted. Statistical error in the frequency measurements was under 1 MHz.

To measure the relative intensities, we estimated the depth of the inversion line dip on the oscilloscope over ten trials, taking the average result. We were only able to measure reliable relative intensity data for the three strongest lines as shown in Figure 4. Weaker lines only showed up as a minor blip on the oscilloscope and there-

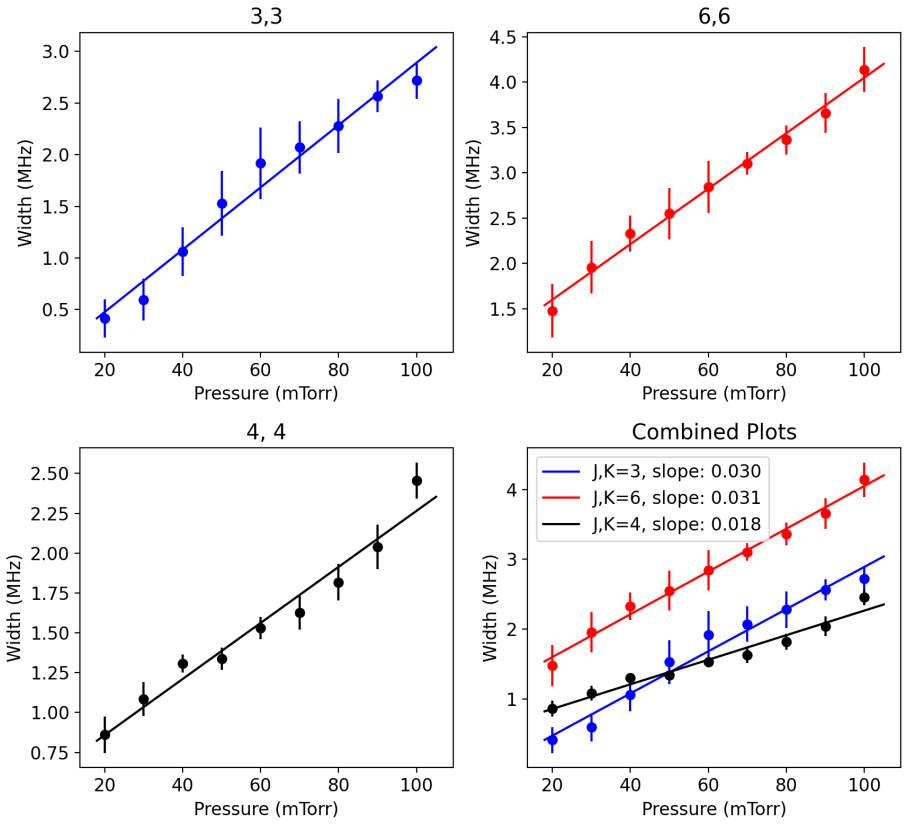

FIG. 6. Absorption broadening as a function of pressure. All broadening appears linear in pressure, though the slope of the (4,4) line is lower than the others. All error bars are two sigma, with sigma estimated using the variation in measurements from trial to trial adjusted for the sample size.

fore were impossible to accurately measure. These data also closely align with the literature.

B. Confidence Intervals / Significance

Before the experiment, we proposed that there was likely to be a large systematic error in measuring the frequency of the microwaves, given that the meter had not been calibrated in a long time. However, with an average residual of just 7 MHz, this error did not play a substantial role. We noticed that the GDO emitted frequencies that were materially different than what the lab manual read (up to 500 MHz), but this source of error did not affect the experiment because we measured frequencies using the cavity, not the setting on the microwave emitter. Our statistical error measured across multiple trials for frequency measurements was under 1 MHz, and there does not seem to have been a large systematic error. There was imprecision in measurements of around 20 MHz in picking out the precise point on the oscilloscope that referenced the center of the dip.

Measuring the relative intensities also had introduced substantial error, resulting in the need for ten trials. Each measurement had to be rounded to the nearest .5 mV on the oscilloscope, and variation from measurement to measurement was as high as 40%. Moreover, different flattening settings substantially changed the strength of the signal and thus the relative intensity. This problem was unavoidable given that the weakest line was invisible without changing the structure of the cavity. Nonetheless, our results closely match the literature when taking into account statistical error.

C. Hyperfine Splitting

The nitrogen atom in ammonia has a nuclear quadrupole moment, which can interact with the electric charge distribution of the rest of the molecule [7]. Thus, there are four extra terms in the Hamiltonian, which creates two smaller frequencies at which absorption also occurs (because the resulting energies are slightly shifted) [8]. On the strongest line with $(J, K) = (3, 3)$, we observed hyperfine splitting, as can be seen in Figure 5.

V. PRESSURE BROADENING

A. Results

The width of the absorption spectrum depends on pressure due to the phenomenon known as pressure broadening. At higher pressures, more ammonia molecules collide with one another. These collisions disrupt the energy levels of the ammonia molecules [9]. Since collisions are a stochastic process, more pressure widens the risk of plausible outcomes (where the outcome is the number of collisions a molecule experiences in time δt), resulting in a wider range of energies experienced by a significant share of the ammonia molecules.

Figure 6 shows the variation in the width of the absorption lines as a function of pressure. Our full data can be found in Appendix A. We find a strong, linear relationship between pressure and width. Although it is in a different pressure regime, the literature shows similar results Figure 7 [10]. The slope of the accepted results is substantially larger than ours (3.84 MHz/Torr vs. 30 MHz/Torr), though it is possible that the much lower pressure regime changes the slope of the graph.

We were able to measure pressure broadening on the three strongest absorption lines, namely (3,3), (6,6), and (4,4). The dips of weaker absorption lines were too small to achieve accurate measurements. It is notable that the slopes of the curves for (3,3) and (6,6) are the same, whereas (4,4) is substantially different. We took the measurements for (4,4) on a separate day, meaning that we used different flattening calibration settings. These settings impact the measured widths (though not relative widths), so this factor could explain the difference in slopes.

The linear nature of the graphs makes sense when considering the physics of pressure broadening. Doubling the number of ammonia particles (by doubling the pressure) should double the number of collisions, suggesting that the effect of the collisions could increase by a factor of two.

B. Confidence Intervals / Significance

Particularly for the weaker two absorption lines, there was a substantial amount of estimation involved in measuring the width of the lines as a function of pressure. The variation from say 50 mTorr to 60 mTorr on the oscilloscope was indistinguishable in many cases. This effect likely explains the two data points in the (4,4) plot that are off the line by a statistically significant amount.

Secondly and counterintuitively, the starting level of ammonia also affected the results. When we started at 200 mTorr of ammonia and then leveled off to 100, both the size and width of the dip were much larger than if we had just started at 100. To keep the data consistent, we tried to not overshoot 100.

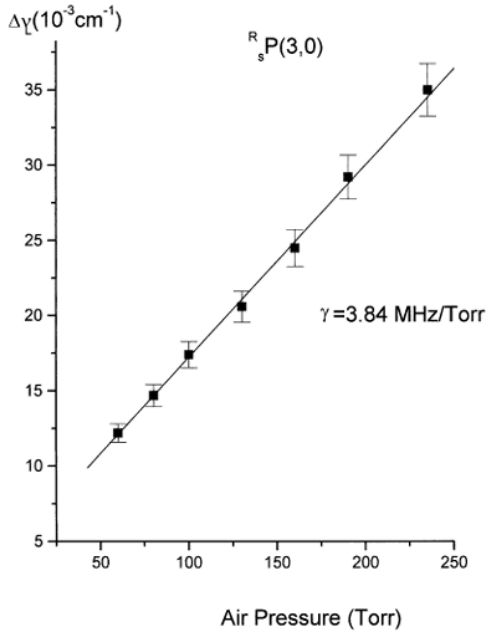

FIG. 7. Accepted pressure broadening values in a different experiment [11]. Though this pressure regime is substantially different than ours, the results are linear.

Beyond these considerations, all pressure readings were 1% measurements or better, so being at a slightly incorrect pressure did not meaningfully change the results.

VI. CONCLUSIONS AND IMPLICATIONS

We have shown that the ammonia molecule is a prime example of quantum tunneling, that its properties can be used to construct an ammonia maser that generates electromagnetic radiation, and that the maser requires almost exact frequencies (see Eqn. 8) for transitions to occur, which is the main principle behind the precision of atomic clocks [6]. By detecting five absorption lines of ammonia, as well as by observing hyperfine splitting for the $(3, 2)$ line, we have shown agreement with accepted experimental values and provided evidence in support of the theory behind ammonia inversion. The maser also has applications to radio astronomy and led to the hydrogen maser, used in GPS systems and in laboratories to control frequencies [12]. Perhaps the most consequential implication of the maser was the proposal of a maser operating at optical frequencies, which is now widely known as the laser [6] [12].

VII. APPENDIX

A. Data Tables

	Frequency reading from cavity	23.878 GHz	23.877 GHz	23.878 GHz	23.876 GHz	23.877 GHz		23.877 GHz	23.877 GHz
(J,K)	Pressure (Millitorr)	Trial 1 Width	Trial 2 Width	Trial 3 Width	Trial 4 Width	Trial 5 Width		Average	Median
(3,3)	20	0.6	0.4	0.2	0.2	0.2		0.32	0.2
(3,3)	30	0.8	0.4	0.4	0.3	0.4		0.46	0.4
(3,3)	40	1.2	0.8	0.8	0.7	0.6		0.82	0.8
(3,3)	50	1.3	1.6	1.2	1	0.8		1.18	1.2
(3,3)	60	1.6	2	1.4	1.2	1.2		1.48	1.4
(3,3)	70	1.6	2	1.6	1.4	1.4		1.6	1.6
(3,3)	80	1.7	2.2	1.7	1.6	1.6		1.76	1.7
(3,3)	90	2	2.2	2	1.8	1.9		1.98	2
(3,3)	100	2	2.4	2	2	2.1		2.1	2
		Depth = 0.4 mV	Depth = 0.45 mV	Depth = 0.3 mV	Depth = 0.3 mV	Depth = 0.3 mV		Depth = 0.35 mV	Depth = 0.3 mV
(3,3)	5 more Depth trials at 100 Millitorr:	Depth = 0.4 mV	Depth = 0.2 mV	Depth = 0.25 mV	Depth = 0.6 mV	Depth = 0.45 mV		Depth = 0.38 mV	Depth = 0.4 mV

	Frequency reading from cavity	25.061 GHz	25.062 GHz	25.062 GHz	25.062 GHz	25.062 GHz		25.062 GHz	25.062 GHz
(J,K)	Pressure (Millitorr)	Trial 1 Width	Trial 2 Width	Trial 3 Width	Trial 4 Width	Trial 5 Width		Average	Median
(6,6)	20	0.6	0.8	0.6	1	1		.8	1
(6,6)	30	0.8	1	1	1.2	1.3		1.06	1
(6,6)	40	1.1	1.2	1.2	1.4	1.4		1.26	1.2
(6,6)	50	1.1	1.4	1.3	1.5	1.6		1.38	1.4
(6,6)	60	1.2	1.6	1.6	1.6	1.7		1.54	1.6
(6,6)	70	1.6	1.7	1.7	1.6	1.8		1.68	1.7
(6,6)	80	1.7	1.8	1.8	1.8	2		1.82	1.8
(6,6)	90	1.8	2	2	1.9	2.2		1.98	2
(6,6)	100	2	2.4	2.2	2.2	2.4		2.24	2.2
(6,6)		Depth = 0.2 mV	Depth = 0.2 mV	Depth = 0.25 mV	Depth = 0.25 mV	Depth = 0.4 mV		Depth = 0.26 mV	Depth = 0.25 mV
(6,6)	5 more Depth trials at 100 Millitorr:	Depth = 0.3 mV	Depth = 0.25 mV	Depth = 0.25 mV	Depth = 0.15 mV	Depth = 0.2 mV		Depth = 0.23 mV	Depth = 0.25 mV

	Frequency reading from cavity	24.141 GHz	24.141 GHz	24.141 GHz	24.141 GHz	24.141 GHz		24.141 GHz	24.141 GHz
(J,K)	Pressure (Millitorr)	Trial 1 Width	Trial 2 Width	Trial 3 Width	Trial 4 Width	Trial 5 Width		Average	Median
(4,4)	20	0.5	0.6	0.6	0.6	0.4		0.54	0.6
(4,4)	30	0.6	0.7	0.7	0.8	0.6		0.68	0.7
(4,4)	40	0.8	0.8	0.8	0.9	0.8		0.82	0.8
(4,4)	50	0.9	0.8	0.8	0.9	0.8		0.84	0.8
(4,4)	60	1	0.9	1	1	0.9		0.96	1
(4,4)	70	1.1	0.9	1	1.1	1		1.02	1
(4,4)	80	1.2	1	1.1	1.2	1.2		1.14	1.2
(4,4)	90	1.2	1.2	1.2	1.4	1.4		1.28	1.2
(4,4)	100	1.6	1.4	1.6	1.5	1.6		1.54	1.6
		Depth = 0.25 mV	Depth = 0.2 mV	Depth = 0.2 mV	Depth = 0.2 mV	Depth = 0.15 mV		Depth = 0.2 mV	Depth = 0.2 mV
(4,4)	5 more Depth trials at 100 Millitorr:	Depth = 0.15 mV	Depth = 0.2 mV	Depth = 0.15 mV	Depth = 0.15 mV	Depth = 0.15 mV		Depth = 0.2 mV	Depth = 0.17

(J,K)	Sample Size	Mean Depth (mV)	Normalized Mean Depth	Normalized Accepted Depth (from Townes Paper)
(3,3)	10	0.365	1	1
(6,6)	10	0.23	0.6712328	0.7018182
(4,4)	10	0.185	0.5068493	0.4981818

[1] NobelPrize.org, Charles h. townes – facts, `https://www.nobelprize.org/prizes/physics/1964/townes/facts/`, accessed: 10 April 2025.

[2] J. P. Gordon, The maser, Scientific American , 42 (1958).

[3] Inversion spectrum of ammonia (2004), microsoft Word Document, NH3_Inversion_2004-ver2-1.doc.

[4] C. H. Townes, *Microwave spectroscopy* (Dover Publications, New York, 1975) Chapter 3: Symmetric-top Molecules, Section 3-1: Introduction and General Features of Rotational Spectra.

[5] C. H. Townes, The ammonia spectrum and line shapes near 1.25-cm wave-length, Phys. Rev. **70**, 665 (1946).

[6] R. P. Feynman, R. B. Leighton, and M. Sands, *The Feynman Lectures on Physics, Vol. III: Quantum Mechanics* (Addison-Wesley, 1965) Chap. 8: The Hamiltonian Matrix and Chap. 9: The Ammonia Maser.

[7] J. M. Jauch, The hyperfine structure and the stark effect of the ammonia inversion spectrum, Phys. Rev. **72**, 715 (1947).

[8] Cazzoli, G., Dore, L., and Puzzarini, C., The hyperfine structure of the inversion-rotation transition jk = $1_0 \leftarrow 0_0$ of nh3 investigated by lamb-dip spectroscopy, AA **507**, 1707 (2009).

[9] C. A. Potter, A. V. Bushkovitch, and A. G. Rouse, Pressure broadening in the microwave spectrum of ammonia, Phys. Rev. **83**, 987 (1951).

[10] H. Aroui, M. Broquier, A. Picard-Bersellini, J. P. Bouanich, M. Chevalier, and S. Gherissi, Absorption intensities, pressure-broadening and line mixing parameters of some lines of NH_3 in the ν_4 band., **60**, 1011 (1998).

[11] H. Aroui, M. Broquier, A. Picard-Bersellini, J. Bouanich, M. Chevalier, and S. Gherissi, Absorption intensities, pressure-broadening and line mixing parameters of some lines of nh3 in the 4 band, Journal of Quantitative Spectroscopy and Radiative Transfer **60**, 1011 (1998).

[12] G. Meijer, Manipulation and control of molecular beams: The development of the stark-decelerator, in *Molecular Beams in Physics and Chemistry: From Otto Stern's Pioneering Exploits to Present-Day Feats*, edited by B. Friedrich and H. Schmidt-Böcking (Springer International Publishing, Cham, 2021) pp. 463–476.